

ARRIVAL DISTRIBUTION OF ULTRA-HIGH ENERGY COSMIC RAYS:  
PROSPECTS FOR THE FUTUREHIROYUKI YOSHIGUCHI<sup>1</sup>, SHIGEHITO NAGATAKI<sup>1,2</sup>, AND KATSUHIKO SATO<sup>1,2</sup>  
hiroyuki@utap.phys.s.u-tokyo.ac.jp  
UTAP-437

## ABSTRACT

We predict the arrival distribution of UHECRs above  $4 \times 10^{19}$  eV with the event number expected by future experiments in the next few years. We perform event simulations with the source model which is adopted in our recent study and can explain the current AGASA observation. At first, we calculate the harmonic amplitude and the two point correlation function for the simulated event sets. We find that significant anisotropy on large angle scale will be observed when  $\sim 10^3$  cosmic rays above  $4 \times 10^{19}$  eV are detected by future experiments. The Auger array will detect cosmic rays with this event number in a few years after its operation. The statistics of the two point correlation function will also increase. The angle scale at which the events have strong correlation with each other corresponds to deflection angle of UHECR in propagating in the EGMF, which in turn can be determined by the future observations. We further investigate the relation between the number of events clustered at a direction and the distance of their sources. Despite the limited amount of data, we find that the C2 triplet events observed by the AGASA may originate from the source within 100 Mpc from us at  $2\sigma$  confidence level. Merger galaxy Arp 299 (NGC 3690 + IC 694) is the best candidate for their source. If data accumulate, the UHECR sources within  $\sim 100$  Mpc can be identified from observed event clusterings significantly. This will provide some kinds of information about poorly known parameters which influence the propagation of UHECRs, such as extragalactic and galactic magnetic field, chemical composition of observed cosmic rays. Also, we will reveal their origin with our method to identify the sources of UHECR. Finally, we predict the arrival distribution of UHECRs above  $10^{20}$  eV, which is expected to be observed if the current HiRes spectrum is correct, and discuss their statistical features and implications.

*Subject headings:* cosmic rays — methods: numerical — ISM: magnetic fields — galaxies: general — large-scale structure of universe

## 1. INTRODUCTION

The AGASA observation of ultra high energy cosmic rays (UHECRs) above  $10^{19}$  eV reveals at least two features. The cosmic-ray energy spectrum does not show the GZK cutoff (Greisen 1966; Zatsepin & Kuz'min 1966) because of photopion production with the photons of the cosmic microwave background (CMB) and extends above  $10^{20}$  eV (Takeda et al. 1998). On the other hand, their arrival distribution seems to be isotropic on a large scale with a statistically significant small scale clustering (Takeda et al. 1999). The current AGASA data set of 57 events above  $4 \times 10^{19}$  eV contains four doublets and one triplet within a separation angle of  $2.5^\circ$ . Chance probability to observe such clusters under an isotropic distribution is only about 1 % (Hayashida et al. 2000).

Recently, the High Resolution Fly's Eye (HiRes; Wilkinson et al. 1999) reports the cosmic ray flux with the GZK cutoff around  $10^{20}$  eV (Abu-Zayyad et al. 2002). At present, it is very difficult to draw a conclusion about the existence or non-existence of the GZK cutoff, because both the two experiments have detected only a handful of events above this energy. On the other hand, there are new large-aperture detectors under development, such as South and North Auger project (Capelle et al. 1998), the EUSO (Benson & Linsley 1982), and the OWL (Cline & Stecker 2000) experiments. The detection or non-detection of the GZK cutoff in the cosmic-ray spectrum remains open to investigation by these future generation experiments.

Potential models of UHECR origin are constrained by their ability to reproduce the measured energy spectrum and the ar-

ival distribution observed by the AGASA. In our recent work (Yoshiguchi et al. 2002a, hereafter Paper I), we perform numerical simulations for propagation of UHE protons in intergalactic space, and examine whether the present AGASA observation can be explained by a bottom-up scenario in which the source distribution of UHECRs is proportional to that of galaxies. We use the Optical Redshift Survey (ORS; Santiago et al. 1995) to construct realistic source models of UHECRs. We can construct realistic source models of UHECRs by using the galaxy sample, because the astrophysical candidates of UHECR sources, such as active galactic nuclei (AGN, Halzen & Zas 1997), gamma-ray bursts (GRB, Waxman 1995, 2000), and colliding galaxies (Cesarsky 1992; Smialkowski, Giller, & Michalak 2002) are in connection with the galaxies. For example, AGNs are considered as supermassive black holes in the centers of the galaxies. A GRB occurs in a galaxy, and so on.

In Paper I, we calculate both the energy spectrum and arrival directions of UHE protons, and compare the results with the AGASA observation. We find that the arrival distribution of UHECRs become to be most isotropic as restricting sources to luminous galaxies ( $M_{\text{lim}} = -20.5$ ). This is because luminous galaxies in the Local Super Cluster (LSC) distribute outward than faint galaxies, contrary to general clusters of galaxies (Yoshiguchi et al. 2002b). However, it is not isotropic enough to be consistent with the AGASA observation, even for  $M_{\text{lim}} = -20.5$ . In order to obtain sufficiently isotropic arrival distribution, we randomly select sources, which contribute to the observed cosmic ray flux, from the ORS sample more lu-

<sup>1</sup> Department of Physics, School of Science, the University of Tokyo, 7-3-1 Hongo, Bunkyo-ku, Tokyo 113-0033, Japan

<sup>2</sup> Research Center for the Early Universe, School of Science, the University of Tokyo, 7-3-1 Hongo, Bunkyo-ku, Tokyo 113-0033, Japan

minous than  $-20.5$  mag, and find that the isotropic arrival distribution of UHECRs can be reproduced in the case that the number fraction of  $\sim 1/50$  of the sample is selected as UHECR sources. In terms of the source number density, this constraint corresponds to  $\sim 10^{-6} \text{ Mpc}^{-3}$ .

We further find that the small scale anisotropy can not be well reproduced in the case of strong extragalactic magnetic field ( $B \geq 10 \text{ nG}$ ). This is because the correlation at small scale between events which originate from a single source is eliminated, or the correlation continues to larger angle scale, due to large deflection when propagating in the EGMF from sources to the earth. Thus, the AGASA observation may imply that UHECRs propagate along nearly straight lines in intergalactic space. If this is true, local enhancement of UHECR sources in the LSC, which is a source model suggested by many authors (Sigl, Lemoine, & Biermann 1999; Lemoine, Sigl, & Biermann 1999; Isola & Sigl 2002; Sigl 2002), may be disfavored because spatial structure of the LSC predicts large scale anisotropy of UHECR arrival distribution. Our conclusion in Paper I is that a large fraction of cosmic rays above  $10^{20} \text{ eV}$  observed by the AGASA experiment might originate in the top-down scenarios, or that the energy spectrum measured by the Hires experiment might be better.

As mentioned above, many future new experiments are under development. These experiments will provide us a large number of data, at least below  $10^{20} \text{ eV}$ , and allow us to discuss the features of the arrival distribution of UHECRs with better statistical significance. In this paper, we predict the arrival distribution of UHECRs above  $4 \times 10^{19} \text{ eV}$  with the event number expected by future experiments in the next few years. We perform event simulations with the source model which can explain the current AGASA observation. It is noted that our prediction is not the exact arrival directions of each UHECR but the statistical features of the arrival distribution, because there are degrees of freedom of randomly selecting the UHECR sources from the ORS sample. At first, we examine how much the future experiments decrease the statistical uncertainty of the cosmic-ray spectrum at the highest ( $\sim 10^{20} \text{ eV}$ ) energies (Marco, Blasi, & Olinto 2003). Next, we calculate the harmonic amplitude and the two point correlation function, and demonstrate that observational constraints on the model of UHECR origin become severer by new experiments. We further investigate the relation between the number of events clustered at a direction and the distance of their source. Such analysis has never performed before. Implications of the results are discussed in detail. Finally, we also predict the arrival distribution of UHECRs above  $10^{20} \text{ eV}$ , which is expected to be observed if the current HiRes spectrum is correct, and discuss their statistical features and implications.

In section 2, we describe our method of calculation. Results are shown in section 3. In section 4, we summarize the main results and discuss their implications.

## 2. NUMERICAL METHOD

### 2.1. Numerical Simulation

This subsection provides the method of Monte Carlo simulations for propagation of UHE protons in intergalactic space. We use the same numerical approach used in Paper I. Detailed explanations are presented in Paper I.

UHE protons below  $\sim 8 \times 10^{19} \text{ eV}$  lose their energies mainly by pair creations and above it by photopion production (Yoshida & Teshima 1993) in collisions with photons of the CMB. The

pair production can be treated as a continuous loss process considering its small inelasticity ( $\sim 10^{-3}$ ). We adopt the analytical fit functions given by Chodorowski, Zdziarske, & Sikora (1992) to calculate the energy loss rate for the pair production on isotropic photons. On the other hand, protons lose a large fraction of their energy in the photopion production. For this reason, its treatment is very important. We use the interaction length and the energy distribution of final protons as a function of initial proton energy which is calculated by simulating the photopion production with the event generator SOPHIA (Mucke et al. 2000).

The EGMF are little known theoretically and observationally. There is the upper limit for the strength and correlation length of the universal EGMF,  $B \cdot l_c^{1/2} < 1 \text{ nG}(1 \text{ Mpc})^{1/2}$ , as measured by Faraday rotation of radio signals from distant quasars (Kronberg 1994). However, simple analytical arguments based on magnetic flux freezing, and large scale structure simulations passively including the magnetic field (Kulsrud et al. 1997) demonstrate that the magnetic field is most likely as structured as are the baryons. The local EGMF as strong as  $\sim 1 \mu\text{G}$  in sheets and filaments of large scale galaxy distribution, such as in the LSC, are compatible with existing upper limits on Faraday rotation (Ryu, Hang, & Biermann 1998; Blasi, Burles, & Olinto 1999). It is suspected that the arrival distribution of UHECRs depends on the fields in the immediate environment of the observer.

However, we show in Paper I that the source number density  $\sim 10^{-6} \text{ Mpc}^{-3}$  is favoured in order to explain the arrival distribution of UHECRs observed by the AGASA. In this case, there is no source in the LSC. We further find that small scale clustering can not be reproduced in the case of strong EGMF ( $B > 10 \text{ nG}$ ). If the local strong EGMF affects the arrival directions of UHECRs, small scale clustering observed by the AGASA will not be obtained. Thus, we assume that the local strong EGMF in the LSC, even if it exists, does not affect the arrival directions of UHECRs, and adopt a homogeneous random turbulent magnetic field with  $(B, l_c) = (1 \text{ nG}, 1 \text{ Mpc})$ .

We assume turbulent magnetic field with power-law spectrum  $\langle B^2(k) \rangle \propto k^{-n_H}$  for  $2\pi/l_c \leq k \leq 2\pi/l_{\text{cut}}$  and  $\langle B^2(k) \rangle = 0$  otherwise, where  $l_{\text{cut}}$  characterizes the numerical cut-off scale. We use  $n_H = -11/3$  corresponding to the Kolmogorov spectrum. Physically one expect  $l_{\text{cut}} \ll l_c$ , but we set  $l_{\text{cut}} = 1/8 \times l_c$  in order to save the CPU time. The universe is covered with cubes of side  $l_c$ . For each of the cubes, Fourier components of the EGMF are dialed on a cubic cell in wave number space, whose side is  $2\pi/l_c$ , with random phases according to the Kolmogorov spectrum, and then Fourier transformed onto the corresponding cubic cell in real space. We create the EGMF of  $20 \times 20 \times 20$  cubes of side  $l_c$ , and outside it, adopt the periodic boundary condition in order to reduce storage data for magnetic field components. Similar methods for the turbulent magnetic fields have been adopted (Sigl, Lemoine, & Biermann 1999; Lemoine, Sigl, & Biermann 1999; Isola & Sigl 2002). In this study, we neglect the effects of the galactic magnetic field. We will conduct studies on its effects in forthcoming paper.

Finally, we explain how the energy spectrum and the arrival directions of UHECRs are calculated. At first, protons with a flat energy spectrum are injected isotropically at a given point within the range of  $(10^{19.5} - 10^{22}) \text{ eV}$ . 5000 protons are injected in each of 26 energy bins, that is, 10 bins per decade of energy. Then, UHE protons are propagated in the EGMF over 1 Gpc for 15 Gyr. Weighted with a factor corresponding to a

$E^{-2}$  power law spectrum, this provides distribution of energy, deflection angle, and time delay of UHECRs as a function of the distance from the initial point. In this paper, we use the distribution of energies and deflection angles integrated over the time delay, assuming that the cosmic ray flux at the earth is stationary. With this distribution, we can calculate the energy spectrum and the arrival directions of UHECRs injected at a single UHECR source. Then, summing contributions from all the sources (see the section 2.2), we obtain the angular probability distributions of UHECRs as a function of their energies. According to this angular probability distributions, we simulate the energy spectrum and the arrival directions of UHECRs.

## 2.2. Source Distribution

In this study, we assume that the source distribution of UHECRs is proportional to that of the galaxies. We use the realistic data from the ORS (Santiago et al. 1995) galaxy catalog. As mentioned in section 1, we show in Paper I that the arrival distribution of UHECRs observed by the AGASA can be reproduced in the case that the number fraction of  $\sim 1/50$  of the ORS galaxies more luminous than  $M_{\text{lim}} = -20.5$  is selected as UHECR sources. We consider only the prediction of this source model throughout the paper. It is unknown how much an ultimate UHECR source contribute to the observed cosmic ray flux. In paper I, we thus consider the two cases in which all galaxies are the same, and they inject cosmic rays proportional to their absolute luminosity. However, we find that the results in the two cases do not differ from each other, as far as we focus on the luminous galaxies as UHECR sources. Accordingly, we restrict ourselves to the case that all galaxies inject cosmic rays with the same amount.

In order to calculate the energy spectrum and the distribution of arrival directions of UHECRs realistically, there are two key elements of the galaxy sample to be corrected. First, galaxies in a given magnitude-limited sample are biased tracers of matter distribution because of the flux limit. Although the sample of galaxies more luminous than  $-20.5$  mag is complete within  $80 h^{-1}$  Mpc, it does not contain galaxies outside it for the reason of the selection effect, where  $h$  is the Hubble constant divided by  $100 \text{ km s}^{-1}$  and we use  $h = 0.75$ . We distribute sources of UHECRs outside  $80 h^{-1}$  Mpc homogeneously, and calculate their amount from the number of galaxies inside it. Second, our ORS sample does not include galaxies in the zone of avoidance ( $|b| < 20^\circ$ ). In the same way, we distribute UHECR sources in this region homogeneously, and calculate its number density from the number of galaxies in the observed region.

## 2.3. Statistical Methods

In this subsection, we explain the three statistical quantities, the harmonics analysis for large scale anisotropy (Hayashida et al. 1999), the two point correlation function for small scale anisotropy, and the correlation value for investigation of the correlation between the events and their sources defined in our previous study (Ide et al. 2001).

The harmonic analysis to the right ascension distribution of events is the conventional method to search for global anisotropy of cosmic ray arrival distribution. For a ground-based detector like the AGASA and the Auger, the almost uniform observation in right ascension is expected. The  $m$ -th harmonic amplitude  $r$  is determined by fitting the distribution to a sine wave with period  $2\pi/m$ . For a sample of  $n$  measurements

of phase,  $\phi_1, \phi_2, \dots, \phi_n$  ( $0 \leq \phi_i \leq 2\pi$ ), it is expressed as

$$r = (a^2 + b^2)^{1/2} \quad (1)$$

where,  $a = \frac{2}{n} \sum_{i=1}^n \cos m\phi_i$ ,  $b = \frac{2}{n} \sum_{i=1}^n \sin m\phi_i$ . We calculate the harmonic amplitude for  $m = 1 - 4$  from a set of events generated according to predicted probability density distribution of arrival directions of UHECRs.

If events with total number  $n$  are uniformly distributed in right ascension, the chance probability of observing the amplitude  $\geq r$  is given by,

$$P = \exp(-k), \quad (2)$$

where

$$k = nr^2/4. \quad (3)$$

The current AGASA 57 events is consistent with isotropic source distribution within 90 % confidence level (Takeda et al. 1999; Hayashida et al. 2000). We therefore compare the harmonic amplitude for  $P = 0.1$  with the model prediction, and estimate the event number at which large scale anisotropy of the UHECR arrival distribution become significant.

The two point correlation function  $N(\theta)$  contains information on the small scale anisotropy. We start from a set of generated events or the actual AGASA data. For each event, we divide the sphere into concentric bins of angular size  $\Delta\theta$ , and count the number of events falling into each bin. We then divide it by the solid angle of the corresponding bin, that is,

$$N(\theta) = \frac{1}{2\pi|\cos\theta - \cos(\theta + \Delta\theta)|} \sum_{\theta \leq \phi \leq \theta + \Delta\theta} 1 \text{ [sr}^{-1}\text{]}, \quad (4)$$

where  $\phi$  denotes the separation angle of the two events.  $\Delta\theta$  is taken to be  $1^\circ$  in this analysis. The AGASA data shows strong correlation at small angle ( $\sim 2^\circ$ ) with  $5 \sigma$  significance of deviation from an isotropic distribution (Takeda et al. 1999; Hayashida et al. 2000).

We use the correlation value, defined in our previous study (Ide et al. 2001), in order to investigate statistically the similarity between the arrival distribution of UHECRs and the source distribution. The correlation value,  $\Xi$ , between two distributions  $f_e$  and  $f_s$ , is defined as

$$\Xi(f_e, f_s) \equiv \frac{\rho(f_e, f_s)}{\sqrt{\rho(f_e, f_e)\rho(f_s, f_s)}}, \quad (5)$$

where

$$\rho(f_a, f_b) \equiv \sum_{j,k} \left( \frac{f_a(j,k) - \bar{f}_a}{\bar{f}_a} \right) \left( \frac{f_b(j,k) - \bar{f}_b}{\bar{f}_b} \right) \frac{\Delta\Omega(j,k)}{4\pi}. \quad (6)$$

Here subscripts  $j$  and  $k$  discriminate each cell of the sky,  $\Delta\Omega(j,k)$  denotes the solid angle of the  $(j,k)$  cell, and  $\bar{f}$  means the average of  $f$ . In equation 5,  $f_e$  and  $f_s$  represent the distribution of the simulated events and the sources, respectively. In this study, the size of the cell is chosen to be  $1^\circ \times 1^\circ$ . The meaning of  $\Xi$  is as follows. By definition,  $\Xi$  ranges from  $-1$  to  $+1$ . When  $\Xi = +1(-1)$ , two distributions are exactly same (opposite). When  $\Xi = 0$ , we can not find any resemblance between two distributions.

## 3. RESULTS

### 3.1. Statistical Significance of the Energy Spectrum at $\sim 10^{20} \text{ eV}$

Before we discuss the future prospect of the UHECR arrival distribution, we examine how much the future experiments decrease the statistical uncertainty of the cosmic-ray spectrum at

the highest energy range ( $\sim 10^{20}$  eV). In figure 1, we show the energy spectrum predicted by a specific source scenario in the case that the number fraction of 1/50 of the ORS galaxies more luminous than  $M_{\text{lim}} = -20.5$  is selected as UHECR sources. The injection spectrum is taken to be  $E^{-2}$ .

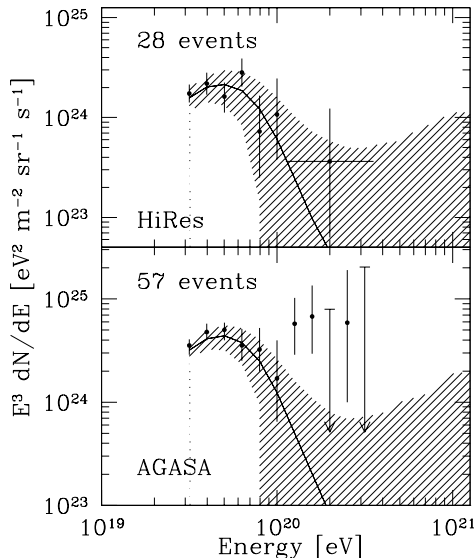


FIG. 1.— Energy spectrum with injection spectrum  $E^{-2}$ , predicted by a specific source scenario in the case that the number fraction of 1/50 of the ORS galaxies more luminous than  $M_{\text{lim}} = -20.5$  is selected as UHECR sources. The simulations are performed with the fixed event numbers above  $4 \times 10^{19}$  eV. The shaded region indicates the statistical error due to the finite number of simulated events. We also show the observed cosmic-ray spectrum by the Hires (Abu-Zayyad et al. 2002) and the AGASA (Hayashida et al. 2000).

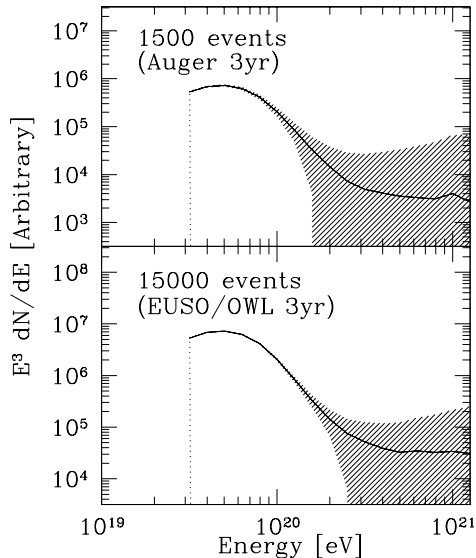


FIG. 2.— Same as figure 1, but with the total number of events expected by 3 year operation of the Auger and the EUSO/OWL.

Berezinsky, Gazizov, & Grigorieva (2002) show that predicted flux of UHECRs fall short of the observed flux below  $10^{19.5}$  eV in the case of injection spectrum  $E^{-2}$ . However, there

may be UHECR production sites in which maximum energy of cosmic ray achieved is lower than  $10^{19.5}$  eV. These components may substantially contribute to the cosmic ray flux below  $10^{19.5}$  eV. Throughout the paper, we assume that these components bridge the gap between the observed flux and the predicted one with the injection spectrum  $E^{-2}$ , and restrict ourselves to cosmic rays only above  $10^{19.5}$  eV.

In figure 1, event simulations are performed with the fixed event numbers above  $4 \times 10^{19}$  eV. Typically, we perform 10000 such simulations. The shaded region indicates the statistical error due to the finite number of simulated events. The spectrum measured by the HiRes is consistent with our model prediction, while that of the AGASA is not. However, the statistical significance of deviation from the prediction of our source scenario is about only  $\sim 2\sigma$ . The region of the energy spectrum dominated by statistical fluctuation is moved to higher energies with increasing the data, as shown in figure 2. It is noted that the future experiment, such as the Auger and the EUSO/OWL, would detect  $\sim 500$  and  $\sim 5000$  events above  $4 \times 10^{19}$  eV per year, respectively. This high statistics will allow us to conclude the presence or absence of the GZK cutoff in the cosmic-ray spectrum in the next few years. Similar conclusion is obtained in Marco, Blasi, & Olinto (2003).

### 3.2. Arrival Distribution of UHECRs above $4 \times 10^{19}$ eV

In this subsection, we present the results of the numerical calculations for the arrival distributions of UHECRs. Figure 3 shows realizations of the UHECR arrival direction above  $4 \times 10^{19}$  eV predicted by a specific source scenario in the case that the number fraction of 1/50 of the ORS galaxies more luminous than  $M_{\text{lim}} = -20.5$  is randomly selected as UHECR sources. Distribution of selected sources within 200 Mpc is also shown as circles of radius inversely proportional to their distances. Only the sources within 100 Mpc are shown with bold lines. Throughout the paper, we show the results only for this specific source scenario. We have checked that the results do not depend very much on the realization of the source selection, unless extremely nearby sources ( $< 30$  Mpc) are accidentally selected. We note that the current AGASA data set include 49 events with energies of  $4 \times 10^{19} - 10^{20}$  eV in the range of  $-10^\circ \leq \delta \leq 80^\circ$ . This event number corresponds to 100 events in figure 3, where we do not restrict the arrival directions of UHECRs in any range of  $\delta$ .

A visual inspection of figure 3 reveals no significant large scale anisotropy. We show the harmonic amplitude as a function of the event number for  $m = 1 - 4$  in figure 4. We plot the average over all trial of the event realizations from the calculated probability distribution with the statistical error. In order to obtain the average and the variance, we dial the simulated sets of events 20 – 1000 times depending on the total event number. The region below the solid line in this figure is expected from the statistical fluctuation of isotropic source distribution with the chance probability larger than 10%. Of course, this region become smaller with increasing the event number.

At present, our source model predicts the harmonic amplitude consistent with the isotropic source distribution. However, future experiments will separate our model prediction from the isotropic source at the confidence level of 90% with the event number of the order  $\sim 10^3$ . It is also found that the amplitude for  $m = 1$  is smaller than that for another values of  $m$ . The amplitude for larger  $m$  quantifies anisotropy on smaller scale. Therefore, this dependence on  $m$  reflects the fact that the arrival

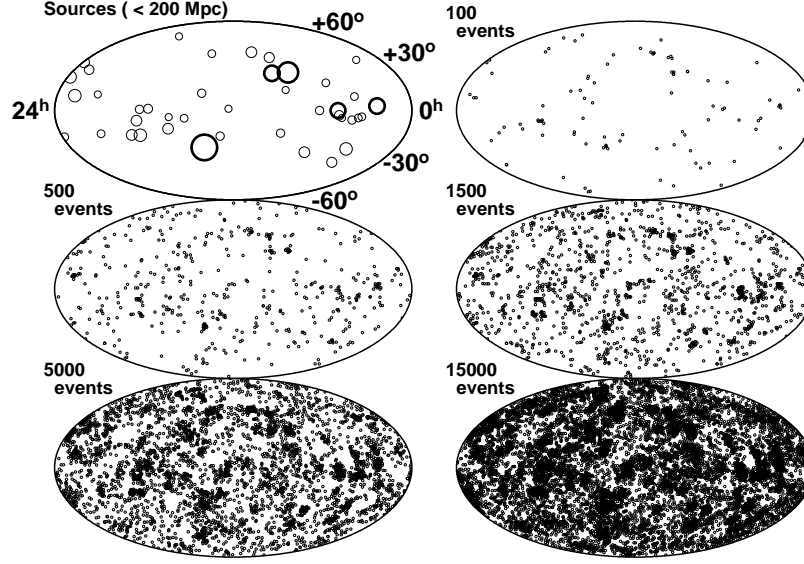


FIG. 3.— Realizations of arrival directions of UHECRs above  $4 \times 10^{19}$  eV predicted by a specific source scenario in the case that the number fraction of  $1/50$  of the ORS galaxies more luminous than  $M_{\text{lim}} = -20.5$  is selected as UHECR sources. Distribution of selected sources within 200 Mpc is also shown as circles of radius inversely proportional to their distances. Only the sources within 100 Mpc are shown with bold lines.

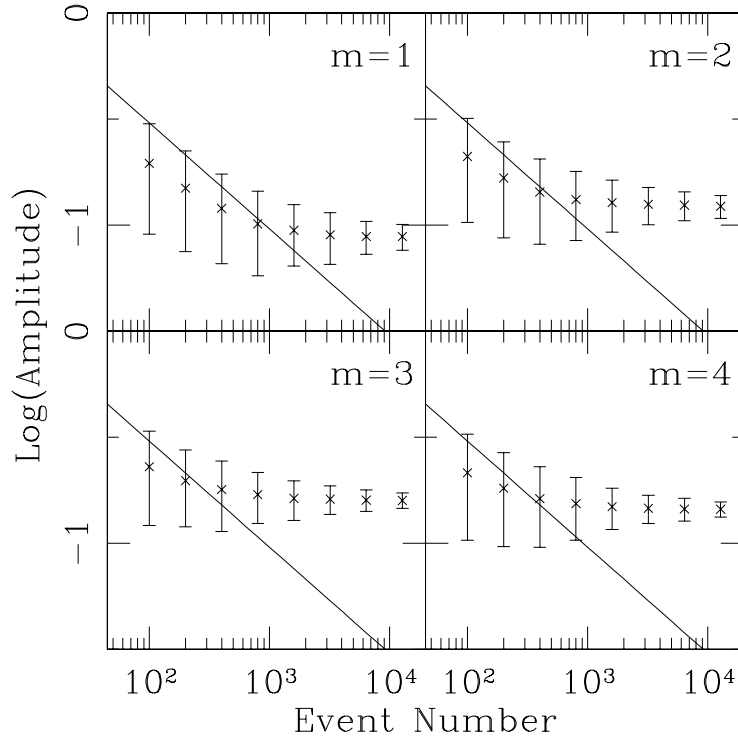


FIG. 4.— Harmonic amplitude predicted by a source model of Figure 3 as a function of the total number of events. The errorbars represent the statistical fluctuations due to the finite number of the simulated events. The region below the solid line is expected from the statistical fluctuation of isotropic source distribution with the chance probability larger than 10%.

distribution shown in figure 3 becomes to reveal the distribution of their sources with increasing the event number, in the manner that the event clusterings occur at the directions of the nearby ( $< 100$  Mpc) sources. This feature of the UHECR arrival distribution is discussed below in detail.

In this source scenario, the small scale anisotropy observed by the AGASA is also reproduced, as is evident from figure 5, where the two point correlation functions of the simulated events are shown. The errorbars represent the statistical fluctuations due to the finite number of the simulated events. For the event number of 100, we also show the two point correlation function on the AGASA 49 events in the energy range of  $4 \times 10^{19} - 10^{20}$  eV, multiplied by factor 2 in order to compensate the difference of the range of  $\delta$  between the observation and the numerical calculation. Slight shrinkage of  $N(\theta)$  at the smallest angle bin is due to manner of dividing the sphere into concentric bins when taking the data of numerical simulations of UHECR propagation.

Since the small scale anisotropy is due to the point-like nature of UHECR sources, the angle scale at which there is strong correlation between the events corresponds to the deflection angle of UHECRs in propagation in the EGMF from sources to the earth. Figure 5 demonstrates that, for the amount of data expected with next generation experiments, the statistical uncertainty will considerably decrease. This clarify the angle scale at which the events have strong correlation with each other. Accordingly, we will be able to determine the strength of the universal EGMF from the two point correlation function of observed UHECRs with the sufficient amount of data.

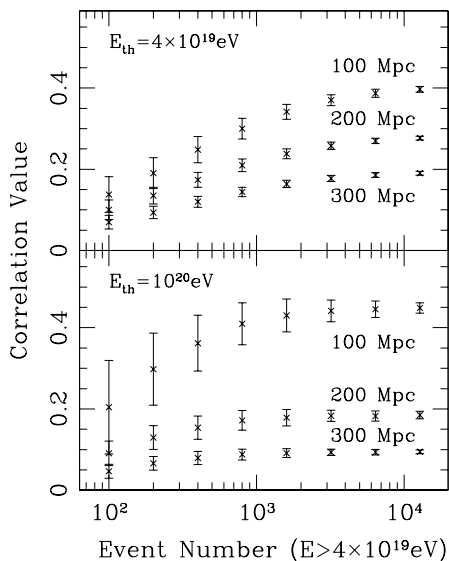


FIG. 6.— Correlation value between the simulated events above  $4 \times 10^{19}$ ,  $10^{20}$  eV and the source distribution of Figure 3. The results are shown for the sources within 100, 200, and 300 Mpc from us. The errorbars represent the statistical fluctuations due to the finite number of the simulated events.

As mentioned above, our source model predicts the statistically significant small scale anisotropy, which correlate with the sources located within 100 Mpc, with a large number of data (see, figure 3). What is deduced from this feature on the origin of UHECRs? To begin with, we quantitatively examine the relation between the event distribution and the source distribution. The upper panel of figure 6 shows the correlation value defined in section 2.3 between the distribution of events above

$4 \times 10^{19}$  eV and the distribution of sources within 100, 200, and 300 Mpc as a function of the event number. The results for the events above  $10^{20}$  eV are discussed in the next subsection. The errorbars are same ones as that in Figure 4.

Clearly visible in this figure is that the correlation of the event distribution with the sources are strongest for the sources within 100 Mpc. This strong correlation is due to the event sets which cluster in the direction of the sources within 100 Mpc (See Figure 3). The number of clustered events fluctuates every realizations, and this number is a critical factor for the correlation with the sources within 100 Mpc. On the other hand, this number do not affect the correlation with the sources within larger distances very much, because there are a number of sources in this case. Therefore, the statistical error is smaller for the correlation with the sources at larger distances. When the event number is close to the order of several  $\times 10^3$ , the correlation values begin to converge, and the final values can be estimated. We emphasize that the expected event rate by the Auger observation is  $\sim 500$  per year. After several years from the operation of the Auger, we would be able to know the source distribution within  $\sim 100$  Mpc.

Here we note that the UHECR sources outside  $107 (= 80h^{-1})$  Mpc in our model are randomly distributed, as mentioned in section 2.2. We should compare the results of the correlation function between the simulated events and the actual galaxy distribution with that between the observed events and the actual galaxy distribution. For the reason of the flux limit, we can not do so using the ORS galaxy sample. However, there is the galaxy survey with a limiting magnitude much deeper than that of the ORS, Sloan Digital Sky Survey (SDSS, Stoughton et al. 2002). We conducted a study of the galaxy number density based on a comparison of the observed number counts between the ORS and the SDSS Early Data Release (Yoshiguchi et al. 2002b). As data obtained by the SDSS accumulate, we will be able to know the actual galaxy distribution of much larger volume, and make precise comparisons between numerical calculations and the observations.

In order to further investigate the relation between the number of the clustered events and the source distance, we calculate the number of events above  $4 \times 10^{19}$  eV within  $2.5^\circ$  from the direction of each source of Figure 3. The angle  $2.5^\circ$  roughly corresponds to both the observational error of arrival directions and the deflection angle of UHECR when propagating in the EGMF ( $B = 1\text{ nG}$ ) over  $\sim 100$  Mpc. The result is shown in Figure 7. The solid angle of the observer viewed from distant sources are inversely proportional to the square of the distance. Thus, contribution to cosmic-ray flux from a source closer to our galaxy is larger than that from a distant source. This is reflected in Figure 7, where the event number at the direction of nearby sources are larger than that of distant sources. A source at  $\sim 280$  Mpc which have larger number of event in its direction happens to be located at the direction of a closer source.

We again note that the event number 100 corresponds to the observed one by the AGASA experiment. From figure 7, there must be a source at the direction of triplet event sets within 100 Mpc from us at  $2\sigma$  confidence level. This implies that the triplet observed by the AGASA would originate from sources within 100 Mpc. Indeed, Smialkowski, Giller, & Michalak (2002) show that there are merger galaxies Arp 299 (NGC 3690 + IC 694) at the direction of the AGASA triplet at  $\sim 70$  Mpc. Considering the analysis presented here, Arp 299 is the best candidate of the UHECR source.

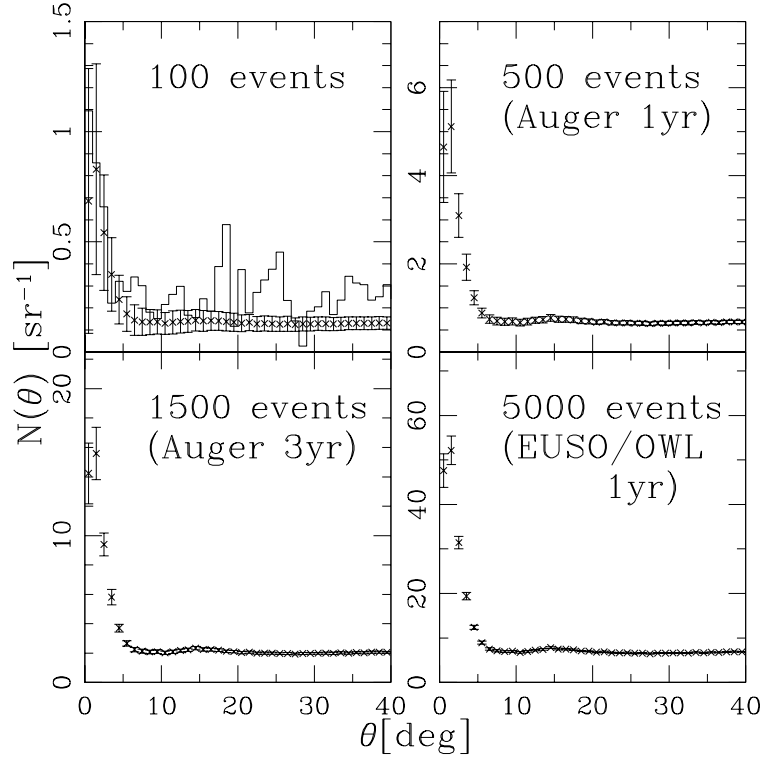


FIG. 5.— Two point correlation functions predicted by a source model of Figure 3. The errorbars represent the statistical fluctuations due to the finite number of the simulated events. For the event number of 100, we also show the two point correlation function on the AGASA 49 events in the energy range of  $4 \times 10^{19} - 10^{20}$  eV, multiplied by factor 2 in order to compensate the difference of the range of  $\delta$  between the observation and the numerical calculation.

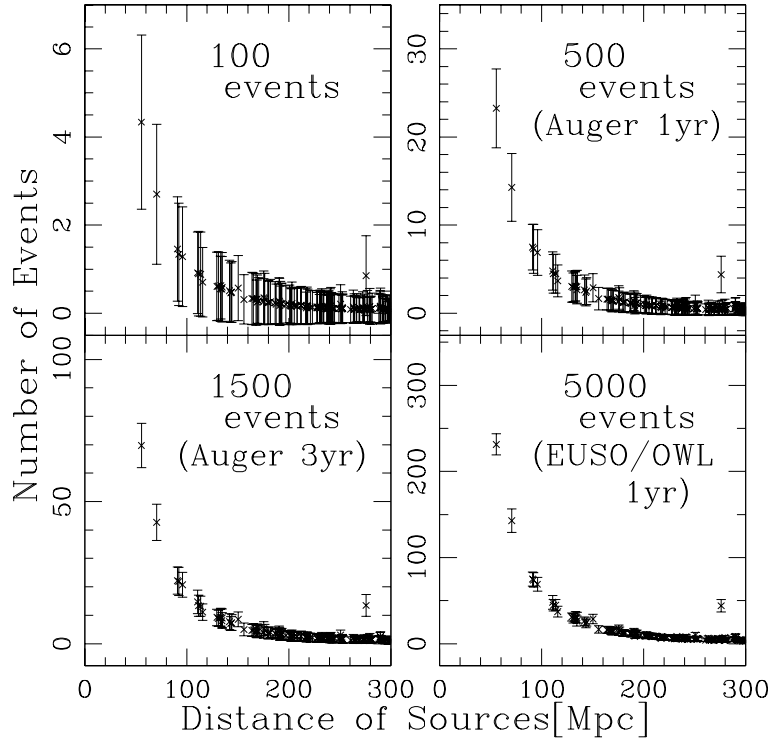


FIG. 7.— Number of events above  $4 \times 10^{19}$  eV within  $2.5^\circ$  from the directions of UHECR sources of Figure 3 as a function of the source distance. The error bars represent the statistical error due to the finite number of simulated events.

Increasing the event number decrease the statistical uncertainty as is evident from figure 7, and thus the relation between the source distance and the number of clustered events in its direction becomes clear. As data accumulate by future experiment, we can know the distance of the source which contributes to a clustered event set by using this relation. Performing this procedure for all the event clusterings, we would be able to determine the distribution of UHECR sources within about 100 Mpc.

### 3.3. Arrival Distribution of UHECRs above $10^{20}$ eV

In this subsection, we present the results of the arrival distribution of UHECRs above  $10^{20}$  eV. It is noted that our source model predicts the cosmic-ray spectrum with the GZK cutoff, unless other components are introduced at this energy range. Accordingly, the features of arrival distributions that we present here are expected to be observed by future experiments if the current HiRes spectrum is correct. If the AGASA spectrum is correct, UHECRs of top-down origin may dominate the cosmic-ray flux at this energy range. However, we may be able to extract UHECRs of bottom-up origin from ones of top-down origin by using the feature of arrival distribution of bottom-up UHECRs, as discussed in the final section.

In figure 8, we show the arrival distribution of UHECRs above  $10^{20}$  eV predicted by the source model of figure 3. This figure is same as figure 3, but only the events with energies above  $10^{20}$  eV are shown. Compared to figure 3, we find that the arrival directions are concentrated in the few directions. This can be also seen from figure 9, which is the same figure as figure 5, but for only UHECRs above  $10^{20}$  eV. At  $\theta > 4^\circ$ , the values of  $N(\theta)$  are almost equal to 0. This is because the sources of UHECRs above  $10^{20}$  eV must be located in a limited volume of radius at most  $\sim 100$  Mpc because of the pion production. Sources at larger distances can not contribute to the cosmic-ray spectrum above this energy.

This feature of the correlation between the events and the sources can be also understood from the lower panel of figure 6. Note that the horizontal axis of this figure is the event number above  $4 \times 10^{19}$  eV. Since the number of events above  $10^{20}$  eV is very small, the statistical error is larger for  $E_{\text{th}} = 10^{20}$  eV than  $E_{\text{th}} = 4 \times 10^{19}$  eV. From this figure, it is clear that the correlation with the sources within 100 Mpc is stronger for  $E_{\text{th}} = 10^{20}$  eV than that for  $E_{\text{th}} = 4 \times 10^{19}$  eV. On the other hand, this dependence becomes opposite in the case of the sources within 200 and 300 Mpc, because UHECRs below  $10^{20}$  eV can come from a much larger volume ( $\sim 1 \text{ Gpc}^3$ ).

We also calculated the harmonic amplitude and the number of events within  $2.5^\circ$  from the directions of the sources for UHECRs above  $10^{20}$  eV. The volume from which UHECRs at this energies can originate is much smaller than that for  $E < 10^{20}$  eV. Although the dependence of the harmonic amplitude on random selection of UHECR sources from the ORS sample is relatively large for this reason, significant anisotropy on large angle scale may be observed when future experiments detect about  $\sim \text{several} \times 10$  cosmic rays above  $10^{20}$  eV. The dependence of the number of events above  $10^{20}$  eV within  $2.5^\circ$  from the directions of the sources on their distances is almost same as that for above  $4 \times 10^{19}$  eV.

## 4. SUMMARY AND DISCUSSION

In this paper, we predicted the arrival distribution of UHECRs above  $4 \times 10^{19}$  eV with the total number of events ex-

pected by next generation experiments in the next few years. We performed event simulations using the ORS galaxy sample to construct a source model of UHECRs, which can explain the current AGASA observation below  $10^{20}$  eV (Paper I). It is noted that our prediction is not the exact arrival directions of each UHECR but the statistical features of the arrival distribution, because there are degrees of freedom of randomly selecting the UHECR sources from the ORS sample and this sample does not contain galaxies outside  $107 (= 80h^{-1})$  Mpc. However, we will be able to know the actual galaxy distribution of much larger volume by using the SDSS galaxy sample (Stoughton et al. 2002) with increasing amount of data.

At first, we calculated the harmonic amplitude and the two point correlation function for the simulated event sets. We found that significant anisotropy on large angle scale will be observed when  $\sim 10^3$  cosmic rays above  $4 \times 10^{19}$  eV are detected by future experiments. The Auger array will detect cosmic rays with this event number in a few years after its operation. The statistics of the two point correlation function will also increase, and the angle scale at which there is strong correlation between the events corresponds to deflection angle of UHECR in propagating in the EGMF. Thus, it is expected that we will be able to know the strength of the EGMF, using the two point correlation function for observed arrival distribution of UHECRs.

Next, we investigated the relation between the number of clustered events and the distance of the source at their direction. We found that the C2 triplet observed by the AGASA (Hayashida et al. 2000) may originate from the source within 100 Mpc from us. Indeed, Smialkowski, Giller, & Michalak (2002) show that there are merger galaxies Arp 299 (NGC 3690 + IC 694) at the direction of the AGASA triplet at  $\sim 70$  Mpc. Considering the analysis presented here, Arp 299 is the best candidate of the UHECR source.

When the event number increases, the statistical uncertainty decreases as is evident from figure 7, and thus the relation between the source distance and the number of clustered events in its direction becomes clear. Using this relation, we will be able to determine the distribution of UHECR sources within about 100 Mpc.

Identification of the sources of UHECRs is extremely important. At first, this will provide some kinds of information about poorly known parameters which influence the propagation of UHECRs, such as extragalactic and galactic magnetic field, chemical composition of observed cosmic rays. Furthermore, this will give an invaluable information on mechanisms and physical conditions which lead to acceleration of cosmic rays to energies of order  $10^{20}$  eV. In particular, we showed that there was the strong correlation between the arrival distribution of UHECR above  $10^{20}$  eV and the source distribution within 100 Mpc. If the cosmic-ray spectrum measured by the HiRes experiment is correct, the UHECR arrival distribution similar to figure 8 will be observed by future experiments. We will be able to know the maximum energies achieved by cosmic rays in each identified object. If the AGASA spectrum is correct, and cosmic-ray flux is dominated by the component of top-down origin. However, the number density of the supermassive particles, whose decay product can be observed UHECRs above  $10^{20}$  eV, is estimated as  $10^{36} \text{ Mpc}^{-3}$  in our galactic halo in order to explain the observed flux, as we discussed in Paper I. In this case, there would be no small scale anisotropy of arrival distribution of UHECRs above  $10^{20}$  eV which are generated by the top-down mechanisms. On the other hand, the arrival direc-



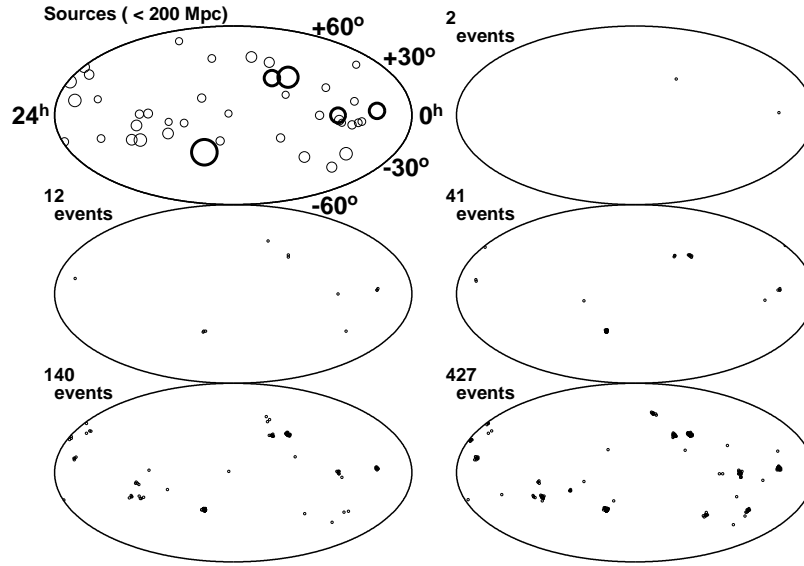


FIG. 8.— Same as figure 3, but only the events with energies above  $10^{20}$  eV are shown.

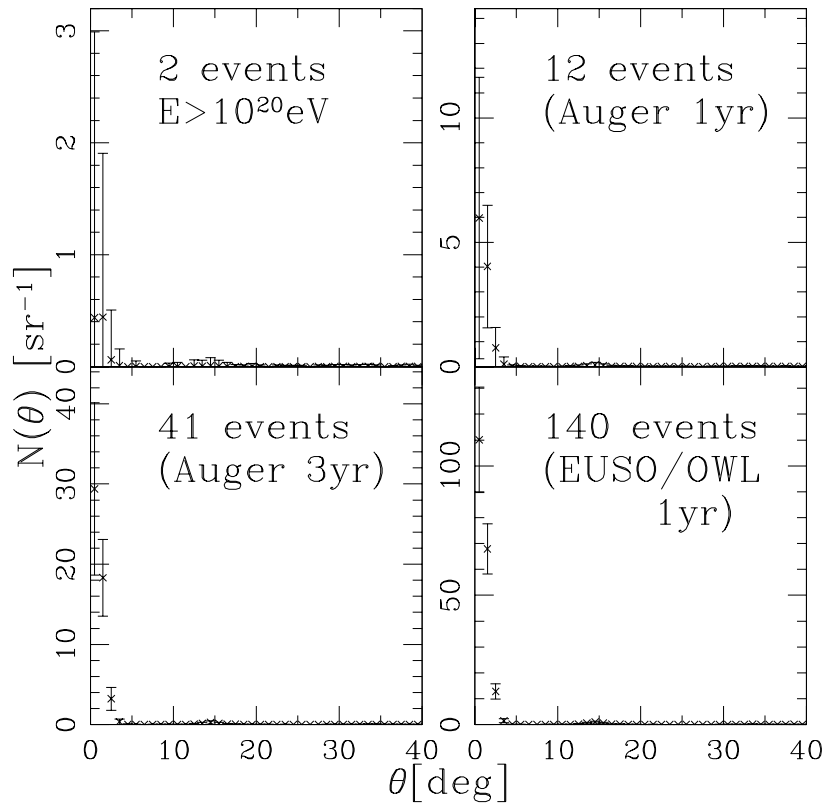


FIG. 9.— Same as figure 5, but only for UHECRs above  $10^{20}$  eV.

tions of bottom-up UHECRs are strongly concentrated in the few directions, as presented in the previous section. We may be able to extract UHECRs of bottom-up origin from ones of top-down origin, and obtain an information on the maximum energies of cosmic rays.

In Paper I, we showed that the number density of UHECR sources may be  $\sim 10^{-6} \text{ Mpc}^{-3}$  in order to explain the UHECR arrival distribution observed by the AGASA experiments. Nevertheless, we could not know which of the astrophysical objects

mainly contributes to the observed cosmic-ray flux. However, with the method to identify the sources of UHECR developed in this paper, we will reveal their origin and obtain an useful information on acceleration mechanism to the highest energy.

This research was supported in part by Giants-in-Aid for Scientific Research provided by the Ministry of Education, Science and Culture of Japan through Research Grant No.S14102004 and No.S14079202.

#### REFERENCES

- Abu-Zayyad T. et al. (The HiRes Collaboration) 2002, astro-ph/0208243  
 Benson R., & Linsley J. 1982, A&A, 7, 161  
 Berezhinsky V., Gazizov A.Z., & Grigorieva S.I. 2002, hep-ph/0204357  
 Blasi P., Burles S., & Olinto A.V. 1999, ApJ, 514, L79  
 Capelle K.S., Cronin J.W., & Parente G., Zs E. 1998, APh, 8, 321  
 Cesarsky C.J. 1992, Nucl. Phys. B (Proc. Suppl.), 28, 51  
 Chodorowski M.J., Zdziarske A.A., & Sikora M. 1992, ApJ, 400, 181  
 Cline D.B., & Stecker F.W. OWL/AirWatch science white paper, astro-ph/0003459  
 Greisen K. 1966, Phys. Rev. Lett., 16, 748  
 Halzen F., & Zs E. 1997, ApJ, 488, 669  
 Hayashida N., et al. 1999 APh, 10, 303  
 Hayashida N., et al. 2000, astro-ph/0008102  
 Ide Y., Nagataki S., Tsubaki S., Yoshiguchi H., & Sato K. 2001, PASJ, 53, 1153  
 Isola C., & Sigl G. 2002, astro-ph/0203273  
 Kronberg P.P. 1994, Rep. Prog. Phys. 57, 325  
 Kulsrud R.M., Cen R., & Ostriker J.P., Ryu D. 1997, ApJ, 480, 481  
 Lemoine M., Sigl G., & Biermann P. 1999, astro-ph/9903124  
 Marco D.D., Blasi P., & Olinto A.V. 2003, astro-ph/0301497  
 Mucke A., Engel R., Rachen J.P., Protheroe R.J., & Stanev T. 2000, Comput. Phys. Commun. 124, 290  
 Ryu D., Kang H., & Biermann P.L., 1998, A&A, 335, 19  
 Santiago B.X., Strauss M.A., Lahav O., Davis M., Dressler A., & Huchra J.P. 1995, ApJ, 446, 457  
 Sigl G., Lemoine M., & Biermann P. 1999, Astropart. Phys., 10, 141  
 Sigl G. 2002, astro-ph/0210049  
 Smialkowski A., Giller M., & Michalak W. 2002, astro-ph/0203337  
 Stoughton C., et al. 2002, AJ, 123, 485  
 Takeda M., et al. 1998, Phys. Rev. Lett., 81, 1163  
 Takeda M., et al. 1999, ApJ, 522, 225  
 Waxman E. 1995, Phys. Rev. Lett., 75, 386  
 Waxman E. 2000, Nucl. Phys. Proc. Suppl., 87, 345  
 Wilkinson C.R., et al. 1999, APh, 12, 121  
 Yoshida S., & Teshima M. 1993, Prog. Theor. Phys. 89, 833  
 Yoshiguchi H., Nagataki S., Tsubaki S., & Sato K. 2002a, ApJ in press (Paper I, astro-ph/0210132)  
 Yoshiguchi H., Nagataki S., Sato K., Ohama N., & Okamura S. 2002b, PASJ in press (astro-ph/0212061)  
 Zatsepin G.T., & Kuz'min V.A. 1966, JETP Lett., 4, 78